

QM study on regioselectivity in the synthesis of pyrimido[4,5-b][1,4]benzothiazines: kinetic and thermodynamic point of view

Mina Ghiasi¹ · Mahmonir Aghawerdi¹ · Majid M. Heravi¹

Received: 4 July 2016 / Accepted: 21 November 2016
© Iranian Chemical Society 2017

Abstract In the present study, the experimentally observed regioselectivity in pyrimido[4,5-b][1,4]benzothiazine synthesis has been modeled using density functional theory method at M06/6-311++G** level. Also the tautomerism of all four tautomers of 6-ethyl-2-thio(1*H*) pyrimidin-(3*H*)-4-one as an important intermediate through the reaction path in pyrimido[4,5-b][1,4]benzothiazine synthesis has been investigated extensively in the gas and solution phase. The stability order of tautomers was found as $A > D > B > C$, in gas and chloroform solvent; however, changing to more polar solvents this order was changed as $A > B > D > C$ using polarized continuum model. In the next step, we focused on another significant feature of this synthesis which has major role in the observed regioselectivity. Two proposed reaction paths with two different transition states that it seems the mode of its intermolecular cyclization has a special role in regioselectivity of the final product have been considered. Comparison of our calculated NMR and IR spectrum with those already reported for some pyrimido[4,5-b][1,4]benzothiazines demonstrates a reliable agreement. Moreover, all obtained results in the gas and solution phase confirm that the synthesis of above-mentioned compound is thermodynamically more favorable than the possible regioisomeric product.

Keywords Pyrimido[4,5-b][1,4]benzothiazine · Tautomerism · Solvent effect · PCM · DFT calculation

Introduction

Pyrimidines, pyrimidinones and their derivatives are diazin heterocyclic compounds with important biological activity and pharmacological properties as effective bactericide and fungicide [1–3]. Pyrimido[4,5-b][1,4]benzothiazines are an important class of fused heterocycles which have been described as being antiviral [4–9], antifungal [10] and enzyme inhibitor [11] agent. It is well known that mammalian lipoxygenases comprise a family of non-heme iron-containing enzymes which catalyze the stereospecific oxygenation of the 5-, 12- or 15-carbon atoms of arachidonic acid [12–14], oxidation of polyunsaturated fatty acids and esters to hydroperoxy derivatives [15]. Among the mammalian lipoxygenase, 15-lipoxygenase (15-LO) is an attractive target for therapeutic intervention [16]. 15-lipoxygenase was implicated in the progression of some cancers [17, 18] and chronic obstructive pulmonary disease [19–21]. There is evidence for the inhibition of 15-LO in the vascular disease treatment, however most compelling [22, 23].

Also we are interested in heterocyclic chemistry [24–31] and more focused on nitrogen heterocycles such as pyrimidine [32, 33] and 1,2,4-triazines [34]. There are two main important concepts in heterocyclic chemistry, tautomerism and regioselectivity.

Tautomers are constitutional isomers of organic compounds that readily interconvert with each other. Tautomerism can play an important role in non-canonical base pairing in DNA and especially RNA molecules [35].

Regioselectivity is the preference of one direction of chemical bond making or breaking of over all other possible directions [36]. As a matter of fact in heterocyclic chemistry, often the generation of a preferential tautomer leads to regioselectivity [37].

✉ Mina Ghiasi
ghiasi@alzara.ac.ir

✉ Majid M. Heravi
mm1331@yahoo.com

¹ Department of Chemistry, Faculty of Physics and Chemistry, Alzahra University, Vanak, Tehran 19835-389, Iran

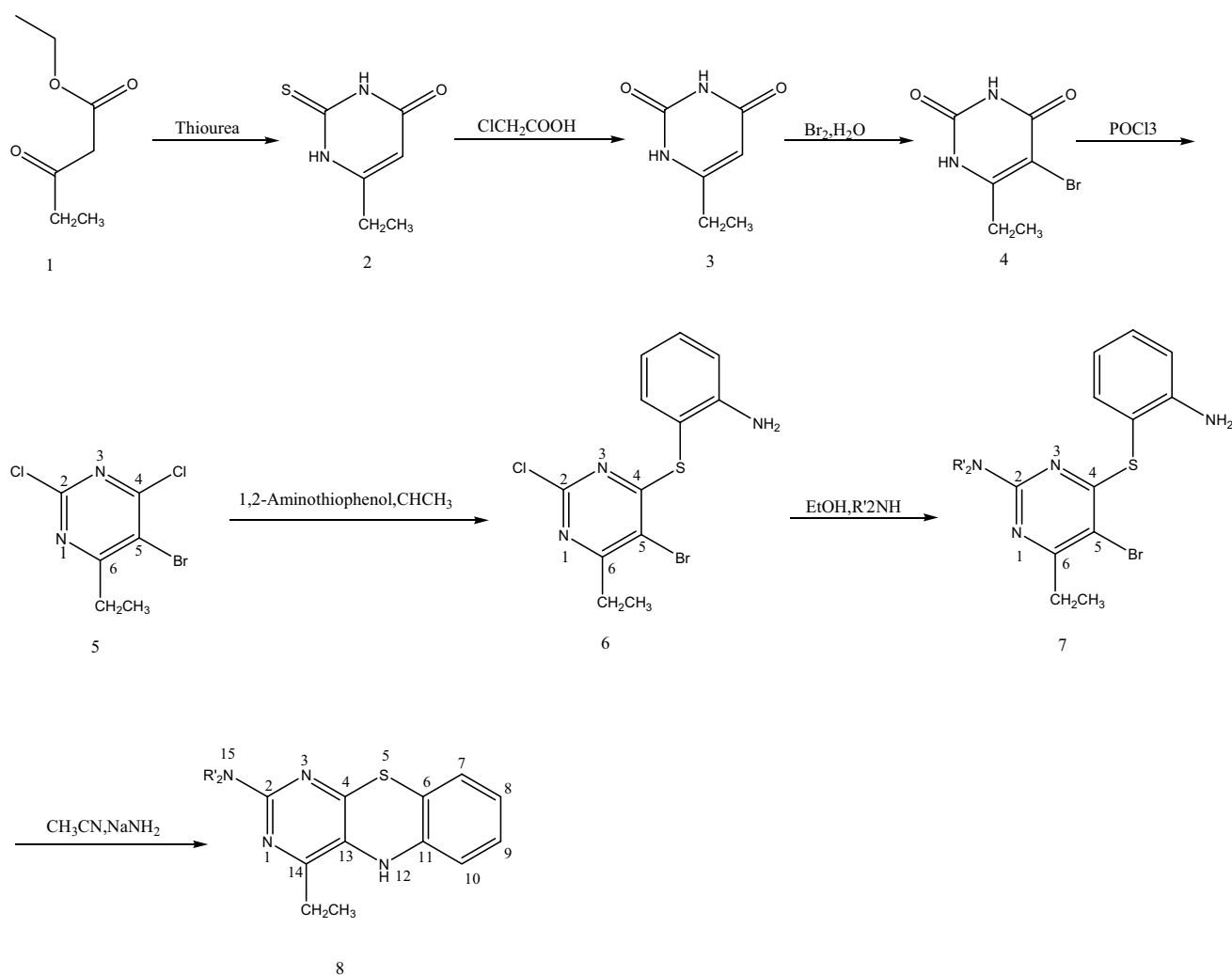


Fig. 1 Schematic representation profile of pyrimido[4,5][1,4]benzothiazines synthesis

In solutions in which tautomerization is possible, a chemical equilibrium of the tautomers will be reached. The exact ratio of the tautomers depends on several factors, including temperature, solvent and pH [38]. However, the ultimate solution for the unprecedented regioselectivity is X-ray crystallography [39].

The computational methods have also been found reliable in this context [40–43], while ago, we computationally studied the tautomerism in 6-substituted, 1,2,4-triazine-3-thion-5-one [42]. Recently, we have studied the base of regioselectivity in Sonogashira synthesis of 6-(4-nitrobenzyl)-2-phenylthiazolo[3,2-b]1,2,4-triazole [44].

Very recently, we justified regioselectivity in our catalytic synthesis of 1,2,3-triazoles, via click reaction based

on computational method [45]. In this context, we reviewed computational studies on the regioselectivity of metal-catalyzed synthesis of 1,2,3 triazoles via click reaction [46].

Armed with these experiences, herein, we wish to reveal our computational study results on the regioselectivity of the synthesis of pyrimido[4,5-b][1,4]benzothiazines.

The reaction pathway is illustrated in Fig. 1. In this scheme, our key step is conversion of compound 5 to compound 6. As a matter of fact, the formation of our target depends on whether which chlorine atom is replaced by aminothiophenol. Basically, the nucleophilic substitution should happen at 2-position more readily than 4-position. However, by elucidation of structure of pyrimido[4,5-b][1,4]benzothiazines 8 it is obvious that chlorine group in 4 position has been replaced selectively. The base of this

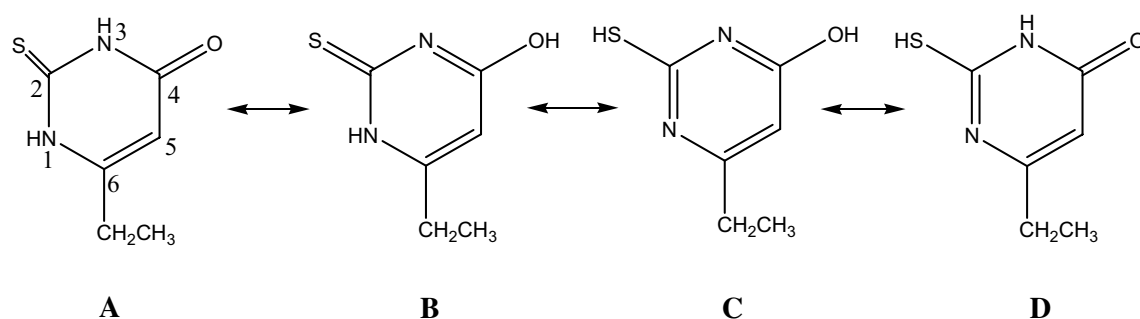


Fig. 2 Possible tautomeric structures of 6-ethyl-2-thio(1*H*) pyrimidin-(3*H*)-4-one (Compound 2), obtained by disposition of the double bonds

selectivity should be looked for in the tautomerism of 2-thio-4-pyrimidone 2. This molecule has four possible tautomers that are caused by prototropism (proton migration), as shown in Fig. 2.

In this research, our attention focuses on mechanistic aspects to achieve a complete understanding on the molecular scale: (1) study on tautomerism of all four 6-ethyl-2-thio(1*H*) pyrimidin-(3*H*)-4-one isomers to extend our knowledge of the tautomeric equilibrium of pyrimidines; (2) computationally investigate the important reasons for the experimentally observed regioselectivity in pyrimido[4,5-*b*][1,4]benzothiazines synthesis from the kinetic and thermodynamic point of view; (3) study of solvent effect on tautomerism, reaction mechanism and calculation of thermodynamic functions. It is noticeable that, despite of pyrimidines importance from pharmacological applications and synthetic point of view, few theoretical studies [49, 50] in this field have been reported. From the computational point of view, accurate information on the structural details and energetic for this synthesis could be an important aspect of addressing the regioselectivity challenge which leads to either kinetic or thermodynamic effects.

Computational details

Ab initio calculations

The geometries and energy of all reactants, intermediates, different tautomers of 6-ethyl-2-thio(1*H*) pyrimidin-(3*H*)-4-one, transition states and products through the reaction path using density functional theory (DFT) [47] with no symmetry constraints have been calculated. The standard 6-311++G** basis set with M06 functional has been introduced as a hybrid meta-GGA (generalized gradient

approximation) exchange correlation functional which was recommended for organometallic and inorganometallic thermochemistry, kinetic investigations, transition state and non-covalent interactions [48]. The QST3 procedure has been used to search for transition states. Intrinsic reaction coordinate (IRC) calculations [49] were employed to ensure the identity of the reactants and products corresponding to each transition structure. Vibrational analyses were performed on all optimized structures with the same functional and basis set as the corresponding geometry optimizations. In addition, the thermodynamic properties of all compounds were obtained from frequency calculations at 298.15 K and 1.0 atmosphere pressure. All reported enthalpies were zero-point (ZPE) corrected with unscaled frequencies. The solvent effects on the conformational equilibrium to evaluate the effects of solvent and contribution to the total enthalpy were investigated with using polarized continuum (overlapping spheres) model (PCM) of Tomasi and coworkers [50]. Solvation calculations were carried out for chloroform, DMSO, ethanol with the geometries optimization for these solvents. All calculations were performed using the Gaussian 98 [51] software.

Calculation of thermodynamic functions

Thermodynamic functions have been calculated from the following equations. Total enthalpies of the studied species *X*, *H*(*X*), at the temperature *T* are usually estimated from Eq. 1 [52, 53].

$$H(X) = E_0 + \text{ZPE} + E_{\text{trans}} + E_{\text{rot}} + E_{\text{vib}} + RT \quad (1)$$

where *E*₀ is the calculated total electronic energy, ZPE stands for zero-point energy, *E*_{trans}, *E*_{rot}, *E*_{vib} are the translational, rotational and vibrational contributions to the enthalpy, respectively. Finally, *RT* represents PV work term and is added to convert the energy to enthalpy.

Table 1 Calculated relative stability energy of 6-ethyl-2-thio(1*H*) pyrimidin-(3*H*)-4-one tautomers in the gas and solution phase at M06/6311++G**

Different phase	ΔE (kcal/mol)			
	A	B	C	D
Gas	0	13.15	18.84	12.74
Chloroform	0	9.57	10.37	5.86
DMSO	0	12.61	19.31	14.94
Ethanol	0	10.86	20.54	17.64

The standard enthalpy change of the reaction ($\Delta H_{\text{reac}}^{\circ}$) is given as:

$$\Delta H_{\text{reac}}^{\circ} = H_{\text{product}} - H_{\text{reactant}} \quad (2)$$

which is the total standard enthalpies of the studied species, at the temperature T estimated from Expression (1).

Similarly, $\Delta S_{\text{reac}}^{\circ}$ could be obtained by

$$\Delta S_{\text{reac}}^{\circ} = S_{\text{product}} - S_{\text{reactant}} \quad (3)$$

According to thermodynamic equation, $\Delta G = \Delta H - T\Delta S$, the $\Delta G_{\text{reac}}^{\circ}$ was calculated.

Results and discussion

According to Fig. 1, the synthesis of pyrimido[4,5-b][1,4] benzothiazines started from 5-bromo-2,4-dichloro-6-ethyl-pyrimidine (compound 5) which was prepared from intermediate key molecule, compound 2 [54]. 6-ethyl-2-thio(1*H*) pyrimidin-(3*H*)-4-one (compound 2) has four possible tautomers, as shown in Fig. 2, that the most stable tautomer contributes to the synthesis profile. So in the first step of this research the geometry and energy of different tautomers of 6-ethyl-2-thio(1*H*) pyrimidin-(3*H*)-4-one are computationally investigated.

Geometry optimization of different tautomers of 6-ethyl-2-thio(1*H*) pyrimidin-(3*H*)-4-one and solvent effect

All four possible tautomers of 6-ethyl-2-thio(1*H*) pyrimidin-(3*H*)-4-one (A–D), which is presented in Fig. 2, were optimized in gas phase and in the different solvent using M06/6-311++G** method. The relative energies of these different tautomers are shown in Table 1. The calculated results show that A tautomer is the most stable tautomer in

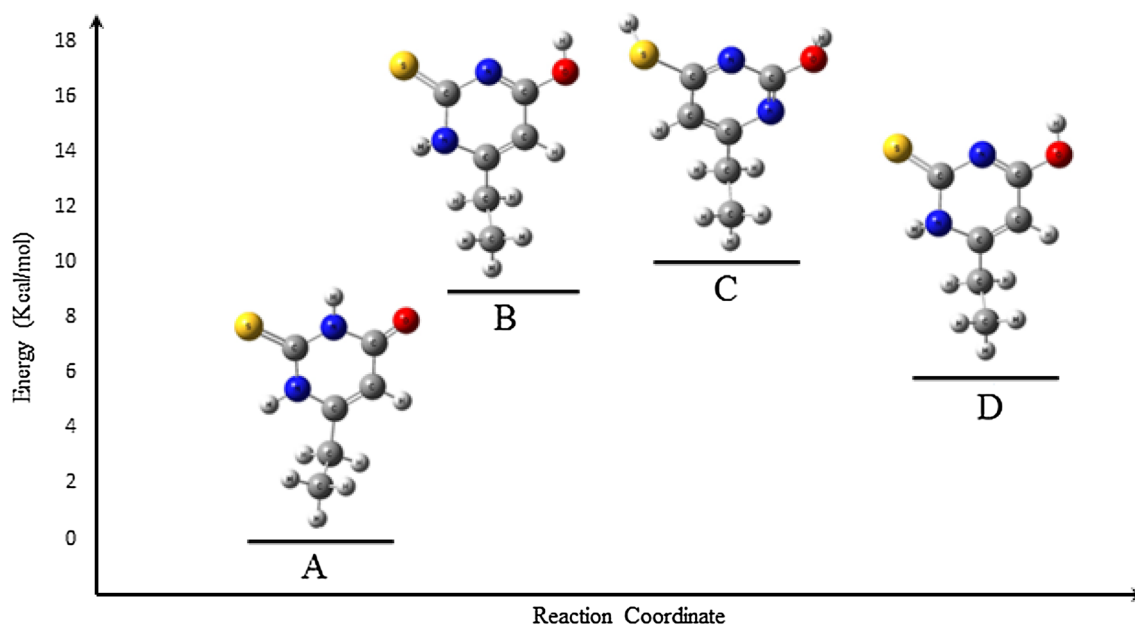
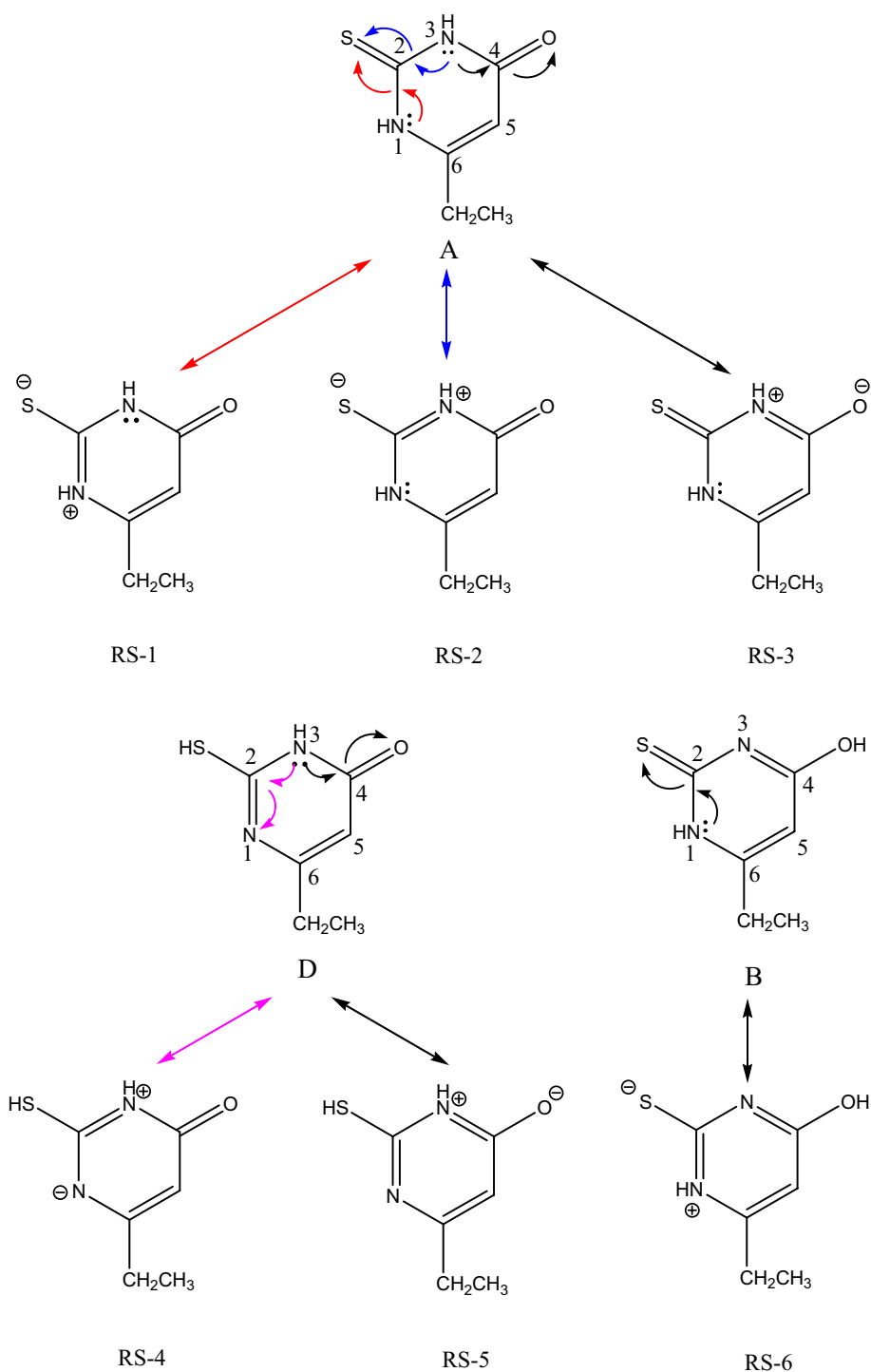
**Fig. 3** Presentation of optimized geometry as well as relative energy of different tautomers of 6-ethyl-2-thio(1*H*) pyrimidin-(3*H*)-4-one in the chloroform at M06/311++G**

Fig. 4 Delocalization of N1 and N3 lone pairs leads to the contribution of different resonance forms in tautomer of 6-ethyl-2-thio(1*H*) pyrimidin-(3*H*)-4-one



gas and in solution phase. Figure 3 presents the optimized geometry of all tautomers with relative stability energy in chloroform solvent. The stability order of different tautomers in gas phase and chloroform is similar: $A > D > B > C$ by 12.74, 13.15 and 18.84 kcal/mol in gas phase, and 5.86, 9.57 and 10.37 kcal/mol in chloroform. But the stability

order in DMSO and ethanol is $A > B > D > C$ by about 12.61, 14.94 and 19.31 kcal/mol and 10.86, 17.64 and 2054 kcal/mol, respectively. As the results indicate, A tautomer is the most stable and C tautomer is the least stable tautomer in all phases. The stability of A tautomer could be caused by cross-conjugation of nitrogen lone pair on

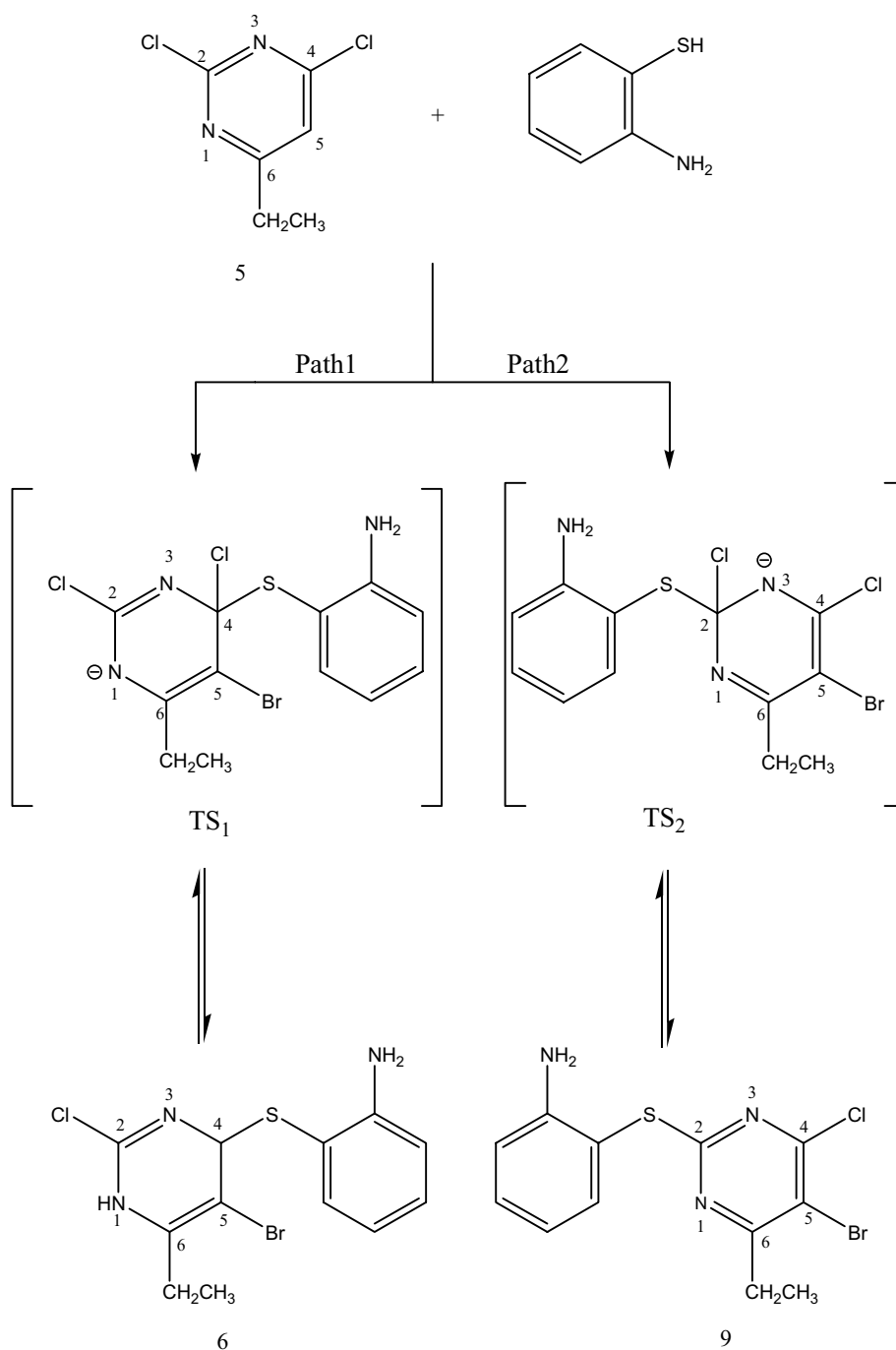
Table 2 Some optimized geometrical parameters of 6-ethyl-2-thio(1*H*) pyrimidin-(3*H*)-4-one tautomers at M06/6-311++G**

Phase	r ₁₂	r ₂₃	r ₃₄	r ₄₅	r ₅₆	r ₁₆	r _{co}	r _{cs}	Θ ₁₂₃	Θ ₂₃₄	Θ ₃₄₅
A											
Gas	1.38	1.37	1.42	1.45	1.35	1.38	1.22	1.67	113.4	127.8	113.4
Chloroform	1.48	1.47	1.46	1.53	1.35	1.47	1.25	1.56	121.8	111.3	120.5
DMSO	1.37	1.36	1.42	1.45	1.35	1.38	1.22	1.66	113.4	127.7	113.4
Ethanol	1.37	1.36	1.42	1.45	1.35	1.38	1.22	1.67	113.4	127.7	113.4
B											
Gas	1.4	1.36	1.32	1.42	1.37	1.36	1.34	1.67	116.1	119.6	125.3
Chloroform	1.47	1.47	1.28	1.53	1.35	1.47	1.43	1.57	121.1	120.1	119.5
DMSO	1.36	1.36	1.31	1.42	1.37	1.40	1.34	1.67	116.2	119.6	125.1
Ethanol	1.40	1.36	1.31	1.42	1.37	1.36	1.34	1.67	116.1	119.6	125.3
C											
Gas	1.33	1.34	1.33	1.40	1.39	1.35	1.35	1.78	127.8	115.3	122.6
Chloroform	1.30	1.47	1.29	1.53	1.35	1.47	1.43	1.78	121.1	120.6	119.3
DMSO	1.33	1.34	1.33	1.40	1.39	1.35	1.35	1.78	127.8	115.3	122.6
Ethanol	1.33	1.33	1.33	1.40	1.39	1.35	1.35	1.78	127.8	115.3	122.6
D											
Gas	1.30	1.36	1.42	1.45	1.37	1.38	1.22	1.78	123.8	123.3	111.7
Chloroform	1.31	1.48	1.47	1.53	1.34	1.47	1.26	1.78	122.4	111.6	119.5
DMSO	1.30	1.36	1.42	1.45	1.37	1.38	1.30	1.78	123.9	123.3	111.7
Ethanol	1.30	1.36	1.42	1.44	1.37	1.38	1.22	1.78	123.9	123.3	111.7

N1 and N3 atoms which lead to three different resonance forms, as shown in Fig. 4 while in the D tautomer delocalization of the N3 lone pair toward C2=N1 or C4=O double bonds results in the contribution of the resonance structures RS-4 or RS-5, respectively. In addition, in B tautomer delocalization of the N1 lone pair toward C2=S double bond results resonance structures RS-6. The comparison between gas and solution phase indicates that a decrease in energy in all tautomers is occurred by changing from the gas phase to polar solvent. This trend refers to molecule with zwitterionic characteristic which makes it favorable to be dissolved in polar protic and aprotic solvents. For the polar protic solvent like DMSO and ethanol, the equilibrium electrostatic interaction between a solvent and solute is more attractive. Therefore, the inclusion of a term accounting for the interaction in the solute Hamiltonian caused an increase in the dipole moment of the solute molecule. But for an aprotic nonpolar solvent, net orientation/polarization induced in the solvent could result in the formation of a reaction field which affects the electronic structure and geometrical parameters of solute molecules. However, cavitation and dispersion energy terms approximately balance

each other, and because of same order and having opposite signs the main contribution of the stabilization of the molecules in solvent phase comes from the solute solvent polarization energy. Results of DFT calculation reveal like in the gas phase the A tautomer is the most stable tautomer in the all solvents, but by changing to more polar solvents stability order is changed: A > B > D > C. As Fig. 3 reveals, D tautomer has two resonance structures (RS-4 and RS-5) in which negative and positive charge lies on N1 and N3 atoms in RS-4 and on O4 and N3 atoms in RS-5 structure, respectively. But B tautomer has one resonance structure RS-6 in that negative charge is resting on S2 atom. The big size of sulfur atom tolerates the negative charge more than O and N atoms; so RS-6 resonance structure is more stabilized in the polar solvent. In addition, changing to more polar solvent the range of stability between most and least stable tautomers varies from ~10 to ~20 kcal/mol. Some selected optimized geometrical parameters of all tautomers are summarized in Table 2. Because of conjugation of C=N, C=S, C=O and C=C double bonds with each other and with nitrogen lone pairs, shortening of some single bonds was observed. For example, N1–C2 (r₁₂) bond length

Fig. 5 Schematic diagram of two different paths in pyrimido[4,5][1,4]benzothiazines synthesis



in D (1.299 Å) and C (1.333 Å) is shorter than same bond in A (1.377 Å) and B (1.404 Å). In addition, the N3–C4 (r_{34}) bond length in B (1.313 Å) and C (1.329 Å) is shorter than similar bond length in A (1.419 Å) that shows double-bond character. The same trends have been observed

when comparing the other bonds with each other and D (1.425 Å). However, no experimental data of this property for 6-ethyl-2-thio(1*H*) pyrimidin-(3*H*)-4-one molecule have been found in the literature in order to make possible comparison.

Fig. 6 Energy profile of displacement of 4-chlorine atom with 2-aminothiophenol at 5-bromo-2,4-dichloro-6-ethylpyrimidine in chloroform solvent (path 1)

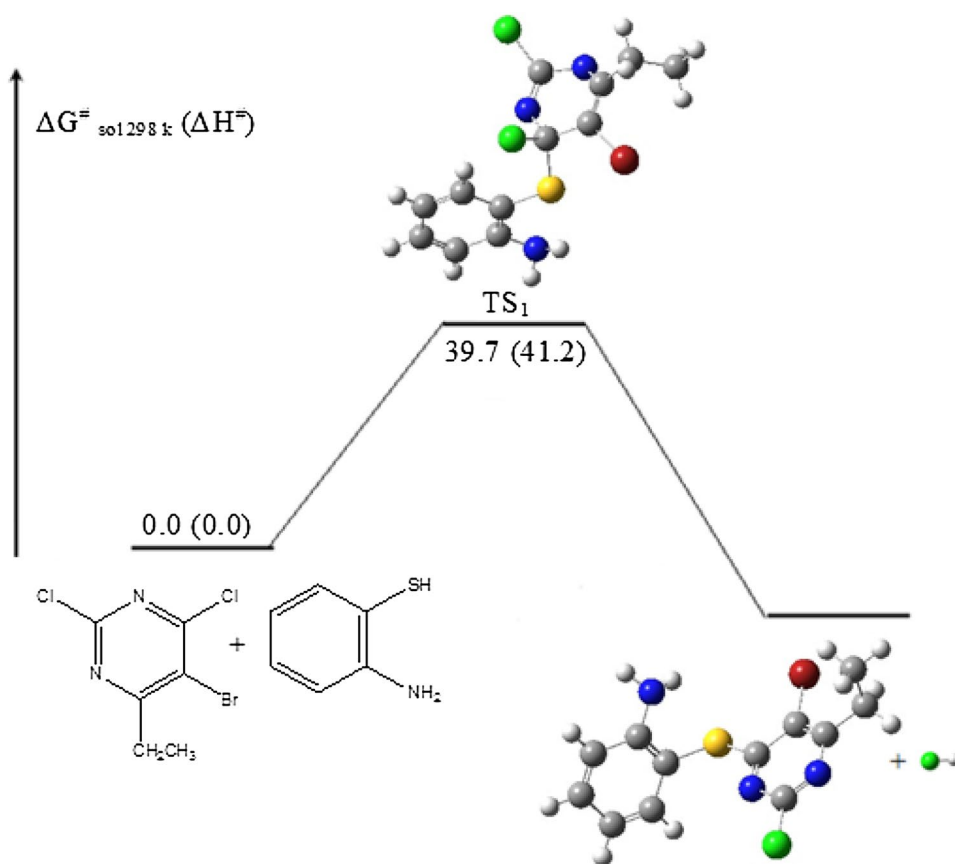


Fig. 7 Energy profile of displacement of 2-chlorine atom with 2-aminothiophenol at 5-bromo-2,4-dichloro-6-ethylpyrimidine in chloroform solvent (path 2)

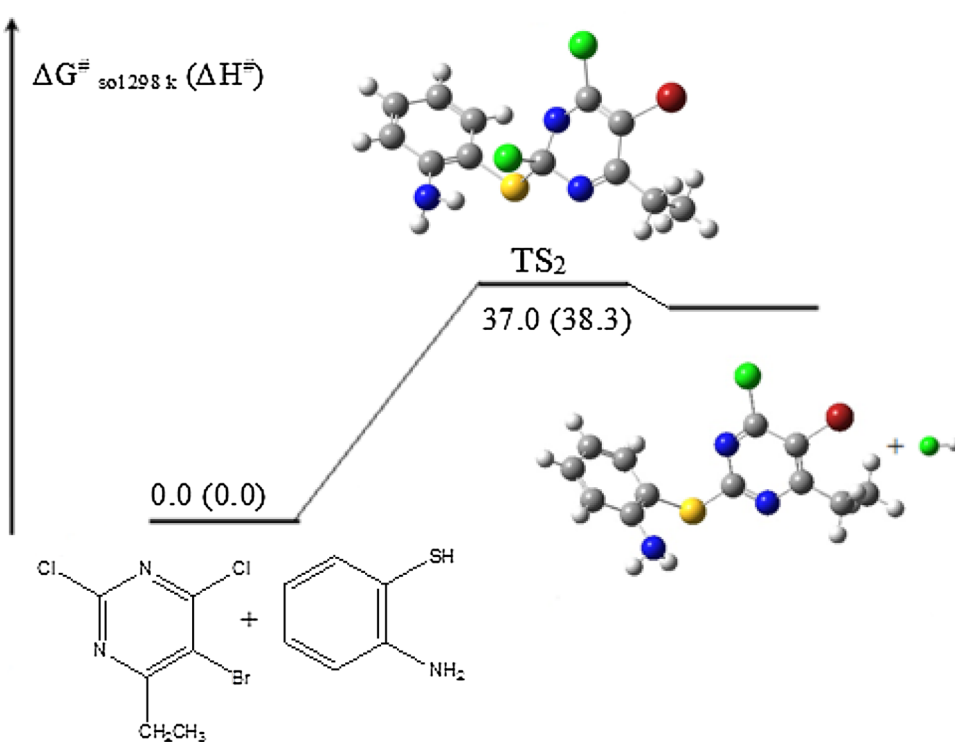


Table 3 Calculated thermodynamic functions during two proposed reaction paths displayed in Fig. 5 at M06/6-311++G** level of theory in the gas phase and chloroform as solvent

Different phase	ΔE°	ΔH°	ΔG°	ΔS°
<i>Path 1</i>				
Gas	−5.77	−5.77	−3.25	−0.0085
Chloroform	−6.40	−6.40	−4.02	−0.0079
<i>Path 2</i>				
Gas	−4.41	−4.41	−2.02	−0.0082
Chloroform	41.95	41.95	44.35	−0.0082

Table 4 Presentation of some structural details of reactant (compound 5), transition states and product according to two proposed reaction paths displayed in Fig. 5 at M06/6-311++G** level of theory in chloroform as solvent

Connected atoms	5	TS1	TS2	6	9
<i>Bond distance (Å)</i>					
C2–N3	1.33	1.30	1.46	1.32	1.48
N3–C4	1.32	1.50	1.76	1.33	1.30
C2–Cl	1.75	1.76	1.76	1.75	–
C4–Cl	1.74	1.76	1.76	–	1.76
C2–S	–	–	1.78	–	1.78
C4–S	–	1.78	–	1.79	–
<i>Bond angle (°)</i>					
N3–C4–Cl	116.26	106.82	121.56	–	120.33
N3–C4–C5	122.38	112.91	116.92	120.61	119.35
C2–N3–C4	115.73	119.39	117.13	116.07	120.65
Cl–C2–N3	115.84	122.72	121.56	115.60	–
<i>Dihedral angle (°)</i>					
Cl–C2–N3–C4	179.76	140.62	73.95	179.72	–
Cl–C4–N3–C2	179.94	98.36	134.60	–	180.00

Reaction profile for synthesis of pyrimido[4,5][1,4]benzothiazines

The reaction of 5-bromo-2,4-dichloro-6-ethyl pyrimidin (compound 5) with 2-amino thiophenol was selected and fully optimized as the model of pyrimido[4,5][1,4]benzothiazines synthesis for DFT calculation. According to Fig. 5, two possible displacements of 4-chlorine atom (path 1) or 2-chlorine atom (path 2) with 2-aminothiophenol are possible in chloroform at room temperature. The representative energy profile of both reaction paths is presented in Figs. 6 and 7. According to Fig. 5, the geometry of both transition states (TS1 and TS2) was constructed and fully optimized. The results of frequency calculation with one imaginary frequency confirm the transition

state. Compounds 6 and 9 have been fully optimized as a product of 4-chlorine and 2-chlorine atom displacement with 2-aminothiophenol, respectively. The resulting energy path renders an exothermic chemical reaction with an activation free energy of 45.05 and 39.70 kcal/mol in the gas phase and in chloroform, respectively, for reaction path 1. Despite reaction path 1, resulting energy profile of path II indicates an endothermic reaction with activation free energy of 42.41 and 37.0 kcal/mol in the gas phase and in chloroform solvent, respectively. Table 3 presents all the calculated thermodynamic functions for the reaction. As the result indicates, however, ΔG° for reaction path 2 is about 3 kcal/mol less than reaction path 1 in gas and solution phase; but since ΔG° reaction to produce of compound 6 in path 1 is negative (−4.02 kcal/mol) and for compound 9 in reaction path 2 is positive (+44.35 kcal/mol), therefore from thermochemical perspective, the reported results in Table 3 clearly proposed that compound 6 is more stabilized, and consequently, its production is more favorable than 9. It is worthwhile to note that this result has been observed previously for this synthesis [54].

The geometry of the transition states, TS1 and TS2, confirms by using IRC and QST3 procedure between reactants and product. Some structural details of reactants, transition state and product are compared in Table 4. The C4–S distance in TS1 (1.53 Å) and C2–S distance in TS2 (1.60 Å) indicate that the nucleophilic attack is a little more advanced in the present case. Furthermore, the distance between C4 and Cl atom increases (~2.65 Å) in the both transition states.

Further the new key intermediate, 2-(5-bromo-6-ethyl-2-substituted-aminopyrimidin-4-ylthio) benzenamines (compound 7) were obtained by the reaction of compound 6 with secondary amines in ethanol according to Fig. 1. Treatment of this intermediate with sodamide in acetonitrile solvent produces pyrimido[4,5-b][1,4]benzothiazines. The energy profile as well as optimized geometry of compound 6, 7 and 8 as a final product (pyrimido[4,5-b][1,4]benzothiazines) is presented in Fig. 8. Also from the thermochemical view point the production of pyrimido[4,5-b][1,4]benzothiazine from compound 6 is exothermic and spontaneous. Since no X-ray data are available for the final product (pyrimido[4,5-b][1,4]benzothiazines), Table 5 demonstrates some structural details of titled compound. To test the accuracy level of our calculations, the proton chemical shifts as well as IR spectra for compounds 6–8 have been calculated.

NMR computations of absolute shieldings were performed using the GIAO method [55] at the DFT optimized structure in the presence of CDCl₃ solvent. The ¹H

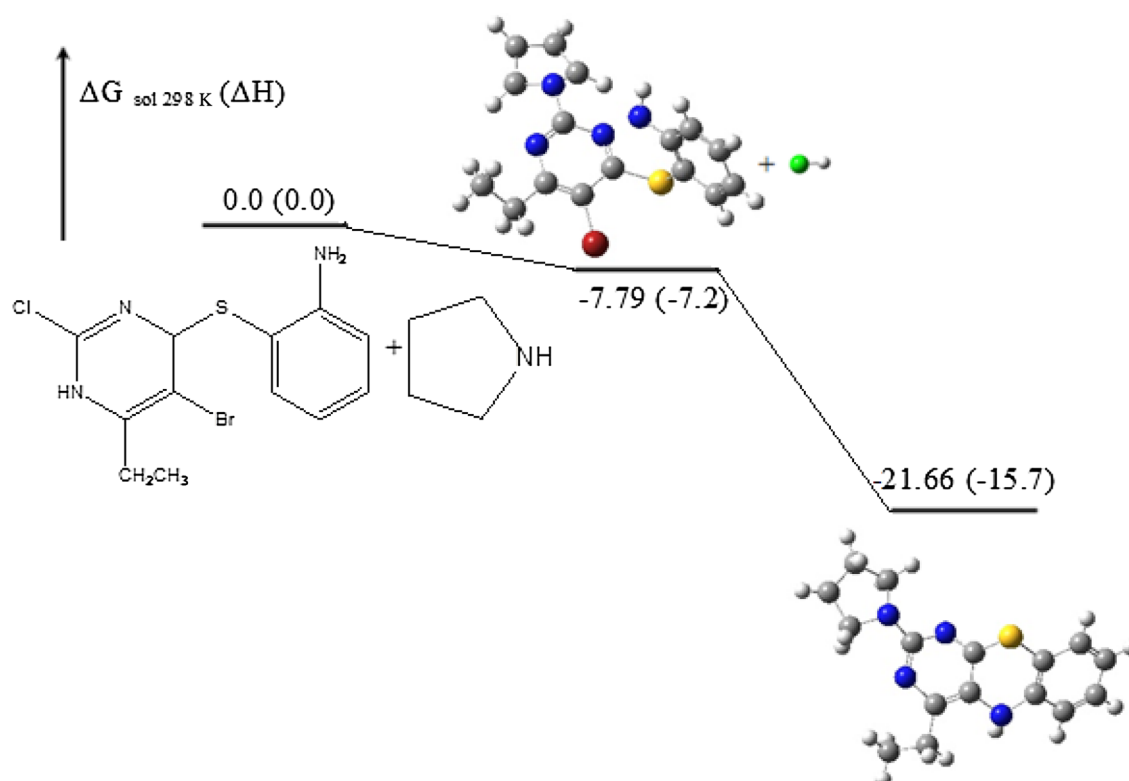


Fig. 8 A comparative illustration for the enthalpy and free energy changes during the regioselective synthesis shown in Fig. 1, calculated at M06/6-311++G** level of theory in solution phase. The

corresponding values of the reaction Gibbs free energy changes have been given in parenthesis

Table 5 Some optimized geometrical parameters of pyrimido[4,5-b][1,4]benzothiazines (compound 8) at M06/6-311++G**

Connected atom	8
<i>Bond distance (Å)</i>	
N1–C2	1.35
C2–N3	1.34
C2–N15	1.36
C13–S	1.78
C4–N5	1.4
N5–C6	1.4
S–C11	1.79
<i>Bond angle (°)</i>	
N1–C2–N3	125.42
N3–C4–C13	123.55
C13–S–C11	100.33
<i>Dihedral angle (°)</i>	
N1–C2–N3–C4	−1.57
S–C13–C4–N5	−0.15

chemical shifts were calculated by using the corresponding absolute shieldings calculated for Me₄Si at the same level of theory (Table 6). The good agreement between

Table 6 Comparison between some experimental chemical shifts (ppm) according to Ref. [28] with calculated results for compounds 6–8

¹ HNMR Chemical shift	Experimental	Theoretical
<i>Compound 6</i>		
H(CH ₂)	2.91	3.10
H(NH ₂)	4.72	4.75
H(aromatic)	6.7–7.5	6.5–7.7
<i>Compound 7</i>		
H(NH ₂)	4.22	4.35
H(aromatic)	6.51–7.42	6.61–7.43
<i>Compound 8</i>		
H(CH ₂)	2.71	2.81
H(aromatic)	6.7–7.6	6.75–7.7
H(NH)	8.40	8.51

experimental and theoretical chemical shifts shows the reliability of DFT calculations for these series of molecules. Further the IR spectra of optimized structure of compound 6, 7 and 8 at the M06/6-311++G** level are calculated. The comparison of theoretical and experimental N–H stretches (Table 7) shows good agreement between them.

Table 7 Comparison between some experimental vibrational wave number (Cm^{-1}) according to Ref. [29] with calculated results for compounds 6–8

IR	Experimental	Theoretical
<i>Component 6</i>		
N–H کشش	3351; 3448	3357–3452
<i>Component 7</i>		
N–H کشش	3362; 3447	3371–3431
<i>Component 8</i>		
N–H کشش	3321	3345

Conclusion

In the present research, We demonstrate the thermodynamical and kinetic study of pyrimido[4,5-b][1,4]benzothiazine synthesis using DFT computational method. In the first step, a systematic study in tautomerism of 6-ethyl-2-thio(1*H*) pyrimidin-(3*H*)-4-one in the gas phase, chloroform, ethanol and DMSO solvent as a key intermediate molecule in synthesis of the final product has undertaken. Further our calculated reaction enthalpies and free energies in gas and solution phase indicate this fact that the production of compound 6 through the reaction path is thermodynamically more favorable than its regioisomer 9. Also from the thermochemical point of view the production of pyrimido[4,5-b][1,4]benzothiazine from compound 6 is exothermic and spontaneous. The validation of our calculated structural and energetic properties of the above-mentioned compound was represented by comparison with the available NMR and IR spectra data that demonstrated a reliable agreement. The present computational studies provide comprehensive understanding on the pyrimido[4,5-b][1,4]benzothiazines synthesis mechanisms as a potent 15-lipoxygenase inhibitor and the annuloselectivity and even guide the future applications of pyrimidin in design of new synthetic strategies for heterocyclic compounds.

Acknowledgements The authors are thankful to Alzahra University Research Council. MMH is thankful also to Iran National Scientific Foundation (INSF) for partial financial support, allocated for his individual research chair.

References

- B. Ramesh, C.M. Bhalgat, *Eur. J. Med. Chem.* **46**, 1882 (2011)
- R. Sawant, V. Sarode, *Iran. J. Pharm. Res.* **10**, 733 (2011)
- V.L. Gein, V.V. Mishunin, E.P. Tsypliyakova, O.V. Vinokurova, M.I. Vakhnin, *Pharm. Chem. J.* **43**, 652 (2009)
- G.R. Revankar, T.S. Rao, K. Ramasamy, D.F. Smee, *Nucleosides Nucleotides* **14**, 671 (1995)
- F.D. Smee, H.A. Alaghmandan, K. Ramasamy, G.R. Revankar, *Antiviral Res.* **26**, 203 (1995)
- D.G. Kini, J.D. Anderson, Y.S. Sanghvi, A.F. Lewis, D.F. Smee, G.R. Revankar, K. Robins, K. Ronald, H.B. Cottam, *J. Med. Chem.* **34**, 3006 (1991)
- E.S.A.M. Badawey, S.M. Rida, A.A. Huzza, H.T.Y. Fahmy, Y.M. Gohar, *Eur. J. Med. Chem.* **28**, 91 (1993)
- P.G. Higgins, G.I. Barrow, D.A.J. Tyrrel, N.J.C. Snell, K. Jones, W.B. Jolley, *Antiviral Chem.* **2**, 61 (1991)
- D.F. Smee, J.H. Huffman, A.C. Gessman, J.W. Huggins, R.W. Sidwell, *Antiviral Res.* **15**, 229 (1991)
- T.S. Rao, G.R. Revankar, R.S. Vinayak, R.K. Robins, *J. Heterocycl. Chem.* **28**, 1779 (1991)
- V.E. Steele, C.A. Holmes, E.T. Hawak, L. Kopelovich, R.A. Lubet, J.A. Crowell, C.C. Sigman, G.F. Kelloff, *Cancer Epidemiol. Biomark. Prev.* **8**, 467 (1999)
- J.M. Schwab, C.N. Serhan, *Curr. Opin. Pharmacol.* **6**, 414 (2006)
- M. Okita, D.C. Gaudette, G.B. Mills, B.J. Holub, *Int. J. Cancer* **71**, 31 (1997)
- M. Croset, N. Brossard, A. Polette, M. Lagarde, *Biochem. J.* **345**, 61 (2000)
- A.R. Brash, *J. Biol. Chem.* **274**, 23679 (1999)
- T. Schewe, *J. Biol. Chem.* **383**, 365 (2002)
- U. Kelavkar, W. Glasgow, T.E. Eling, *Curr. Urol. Rep.* **3**, 207 (2002)
- U.P. Kelavkar, C. Cohen, H. Kamitani, T.E. Eling, K.F. Badr, *Carcinogenesis* **21**, 1777 (2000)
- J. Zhu, I. Kilty, H. Granger, E. Gamble, Y.S. Qiu, K. Hattotuwa, W. Elston, W.L. Liu, A. Liva, R.A. Pauwels, J.C. Kis, V. De Rose, N. Barnes, M. Yeadon, S. Jenkinson, P.K. Jeffery, *Am. J. Respir. Cell Mol. Biol.* **27**, 1044 (2002)
- H.G. Johnson, M.L. McNee, F.F. Sun, *Am. Rev. Respir. Dis.* **131**, 917 (1985)
- A. Brown, A. Henderson, S. Jenkinson, I. Kilty, S. Liu, S. Monaghan, T. Wood, M. Yeadon, *Drugs Future* **27**, C55 (2002)
- L. Zhao, C.D. Funk, *Trends Cardiovasc. Med.* **14**, 191 (2004)
- J.A. Cornicell, B.K. Trivedi, *Curr. Pharm. Des.* **5**, 11 (1999)
- M.M. Heravi, T. Alishiri, *Adv. Heterocycl. Chem.* **113**, 1 (2014)
- M.M. Heravi, B. Talaei, *Adv. Heterocycl. Chem.* **113**, 143 (2014)
- M.M. Heravi, S. Khaghaninejad, M. Mostofi, *Adv. Heterocycl. Chem.* **112**, 1 (2014)
- M.M. Heravi, S. Khaghaninejad, N. Nazari, *Adv. Heterocycl. Chem.* **112**, 183 (2014)
- M.M. Heravi, B. Talaei, *Adv. Heterocycl. Chem.* **114**, 147 (2015)
- M.M. Heravi, V.F. Vavsari, *Adv. Heterocycl. Chem.* **114**, 77 (2015)
- S. Khaghaninejad, M.M. Heravi, *Adv. Heterocycl. Chem.* **45**, 38 (2014)
- M.M. Heravi, V. Zadsirjan, *Adv. Heterocycl. Chem.* **117**, 261 (2015)
- M.M. Heravi, G. Rajabzadeh, F.F. Bamoharram, *J. Mol. Catal. A: Chem.* **256**, 238 (2006)
- M.M. Heravi, S. Sadjadi, H.A. Oskooie, R.H. Shoar, F.F. Bamoharram, *Tetrahedron Lett.* **50**, 662 (2009)
- M.M. Heravi, K. Aghapoor, M.A. Nooshabadi, M.M. Mojtahedi, *Monatsh. Chem.* **128**, 1143 (1997)
- I. Tinoco, C. Bustamante, *J. Mol. Biol.* **293**, 271 (1999)
- B. Andersh, K.N. Kilby, M.E. Turnis, D.L. Murphy, *J. Chem. Educ.* **85**, 1 (2008)
- S. Dadiboyena, E.J. Valente, A.T. Hamme, *Tetrahedron Lett.* **55**, 2208 (2014)
- R.M. Balabin, *J. Chem. Phys.* **131**, 154307 (2009)
- A. Steinbach, A.J. Scheidig, C.D. Klein, *J. Med. Chem.* **51**, 5143 (2008)
- K. Vazdar, M. Vazdar, *Tetrahedron Lett.* **56**, 6908 (2015)
- X. Zhang, *Int. J. Quantum Chem.* **115**, 1658 (2015)
- F.S. Hashemi, F. Forooghian, M.M. Heravi, *THEOCHEM* **770**, 123 (2006)

43. H.R. Memarian, F. Rezaie, H. Sabzyan, M. Ranjbar, J. Iran. Chem. Soc. **11**, 1265 (2014)
44. T. Hosseinejad, M.M. Heravi, R. Firouzi, J. Mole. Model. **19**, 951 (2013)
45. R. Mirsafaei, M.M. Heravi, S. Ahmadi, M.H. Moslemin, T. Hosseinejad, A. Chemical. **402**, 100 (2015)
46. T. Hosseinejad, B. Fattahi, M.M. Heravi, J. Mol. Model. **21**, 1 (2015)
47. R.G. Parr, W. Yang, *Density-Functional Theory of Atoms and Molecules* (Oxford University Press, Oxford, 1989)
48. D.G. Truhlar, Y. Zhao, Theor. Chem. Acc. **120**, 215 (2008)
49. K. Fukui, Acc. Chem. Res. **14**, 363 (1981)
50. V. Barone, M. Cossi, J. Tomasi, J. Comp. Chem. **19**, 404 (1998)
51. M.J. Frisch, G.W. Trucks, H.B. Schlegel, G.E. Scuseria, M.A. Robb, J.R. Cheeseman, V.G. Zakrzewski, J.A. Montgomery, R.E. Stratmann, J.C. Burant, S. Dapprich, J.M. Millam, A.D. Daniels, K.N. Kudin, M.C. Strain, O. Farkas, J. Tomasi, V. Barone, M. Cossi, R. Cammi, B. Mennucci, C. Pomelli, C. Adamo, S. Clifford, J. Ochterski, G.A. Petersson, P.Y. Ayala, Q. Cui, K. Morokuma, D.K. Malick, A.D. Rabuck, K. Raghavachari, J.B. Foresman, J. Cioslowski, J.V. Ortiz, B.B. Stefanov, G. Liu, A. Liashenko, P. Piskorz, I. Komaromi, R. Gomperts, R.L. Martin, D.J. Fox, T. Keith, M.A. Al-Laham, C.Y. Peng, A. Nanayakkara, C.V. Ghonzalez, M. Challacombe, P.M.W. Gill, B.G. Johnson, W. Chen, M. Wong, J.L. Andres, M. Head-Gordon, E.S. Replogle, J.A. Pople, *Gaussian 2003 (Revision-B)* (Gaussian Inc, Pittsburgh, 2003)
52. M. Navarrete, C. Rangel, J.C. Corchado, J. Phys. Chem. A **109**, 4777 (2005)
53. H.Y. Zhang, H.F. Ji, THEOCHEM **667**, 167 (2003)
54. M. Bakavoli, M. Nikpour, M. Rahimizadeh, M.R. Saberi, H. Sadeghian, Bioorg. Med. Chem. **15**, 2120 (2007)
55. K. Wolinski, J.F. Hilton, P.J. Pulay, J. Am. Chem. Soc. **112**, 8251 (1990)